Selective plasma etching of ZrO_x to Si using inductively coupled BCl_3/C_4F_8 plasmas

S. D. Park, J. H. Lim, C. K. Oh, H. C. Lee, and G. Y. Yeom[a)]
Department of Materials Science and Engineering, Sungkyunkwan University, Suwon, Kyunggi-do, 440-746, S. Korea

(Received 22 July 2005; accepted 11 January 2006; published online 3 March 2006)

In this study, the etch characteristics of ZrO_x and the etch selectivity to Si were investigated using BCl_3/C_4F_8 plasmas. The etching mechanism was also investigated. Increasing the C_4F_8 percentage to 4% formed a C–F polymer layer on the silicon surface due to the increased flux ratio of CF_x/F to the substrate, while no such C–F polymer was formed on the ZrO_x surface due to the removal of carbon from CF_x by the oxygen in ZrO_x. By using 3–4% C_4F_8 in the BCl_3/C_4F_8 mixture, infinite etch selectivity of ZrO_x to silicon and photoresist could be obtained while maintaining the ZrO_x etch rate above 400 Å/min. © *2006 American Institute of Physics*. [DOI: 10.1063/1.2180879]

Zirconium oxide (ZrO_x) is an attractive material for use as a gate dielectric for metal-oxide-semiconductor field effect transistors (MOSFETs) and as a storage capacitor for dynamic random access memory (DRAM) devices because it has a high-dielectric constant (~25), wide band gap (4.6–7.8 eV), low-leakage-current, and superior thermal stability.[1,2]

In order to apply ZrO_x to MOSFET and DRAM devices, the ZrO_x films should be patterned by dry etching not only because wet etching cannot delineate high-resolution features but also because ZrO_x can not be removed completely by wet etching due to zirconium silicate ($ZrSi_xO_y$) formation at the ZrO_x and silicon interface[3,4] Dry etching of ZrO_x films requires, not only high ZrO_x etch rates but also high etch selectivities of ZrO_x over the underlying materials such as Si located under the ZrO_x. Until now, a few researchers have investigated the dry etching of ZrO_x using chlorine-based gases, such as Cl_2 (Ref. 5) and Cl_2/BCl_3 (Refs. 3 and 4) for application to MOSFET devices. However, the etch selectivities of ZrO_x over underlying the materials were not high enough (lower than 3.0) because chlorine compounds of silicon show a higher vapor pressure compared to those of ZrO_x in the chlorine-based gas chemistry and, in these etching conditions, the etch rates of ZrO_x were lower than 250 Å/min.

In this letter, in order to obtain higher etch selectivities of ZrO_x over underlying silicon together with high ZrO_x etch rates, ZrO_x etching was carried out using inductively coupled BCl_3/C_4F_8 plasmas. Also, the mechanism obtaining the high etch selectivity was also investigated.

ZrO_x films were etched using an inductively coupled plasma (ICP) equipment that can hold a 6 inch diameter silicon wafer. The ICP source consisted of a gold-coated three-turn coil located on the top of the process chamber separated by a 1 cm thick quartz window. To generate the inductive plasmas, 13.56 MHz radio-frequency (rf) power was applied to the coil, while separate 13.56 MHz rf power was supplied to the substrate to provide a dc bias voltage to the wafer. Substrate cooling was provided by chilled water, therefore, the substrate temperature was kept constant at near room temperature. The distance between the substrate and the source was kept at 100 mm. Details of the ICP system used in the experiment are described elsewhere.[5]

The samples consisted of 3500 Å thick ZrO_x films deposited on *p*-type Si (100) wafers by reactive rf sputtering. The ZrO_x films were patterned with a 1.2 μm thick photoresist (PR) mask. To measure the etch selectivities, PR covered silicon wafers were also etched along with ZrO_x films. BCl_3 (100 sccm) gas was used as the main etch gas and C_4F_8 (0–6 sccm) gas was used as the additive gas. The operating pressure was kept at 12 mTorr. The etch rates were determined using stylus profilometry (Tencor Instrument, Alpha Step 500) of the patterned feature depths before and after stripping the PR. The etch profiles were observed using a field-emission scanning electron microscope (FE-SEM, Hitachi S-4700). The characteristics of the BCl_3/C_4F_8 plasmas during ZrO_x and Si etching were measured by optical emission spectroscopy (OES; SC Technology, PCM420) and the relative OES intensities were measured by adding 5% Ar to the plasmas and by taking the ratio of the OES intensities to the Ar intensity at 750.4 nm. X-ray photoelectron spectroscopy (XPS; Thermo VG, SIGMA PROBE) was also used to analyze the etch products remaining on the etched ZrO_x and Si surfaces. An Al $K\alpha$ source was used to provide monochromatic x rays at 1486.7 eV. The C 1*s* photoelectroemission at 285 eV was used as a reference binding energy.

Figure 1 shows the relative OES intensities of the radicals observed in the BCl_3/C_4F_8 plasmas as a function of C_4F_8 percentage in the BCl_3 (100 sccm)/C_4F_8 (0–6 sccm) gas mixture. The rf inductive power was maintained at 700 W. As shown in the figure, the relative OES intensities of B (249.6 nm), BCl (271.0 nm), and Cl (726.4 nm) in the plasma decreased in general with increasing C_4F_8 due to the decrease in partial pressure of BCl_3 at 12 mTorr of constant operating pressure. In the case of CF_2 (291.2 nm), the intensity increased almost linearly with increasing of C_4F_8, however, in the case of F (704.01 nm), even though the intensity increased significantly initially with the increasing C_4F_8 upto 1.5%, the further increase of C_4F_8 did not change the intensities significantly. The increase of CF_2 with increasing C_4F_8 and the increase of F with the increase of C_4F_8 upto 1.5% are believed to be related to the increase of C_4F_8 partial pressure in the BCl_3/C_4F_8 plasma. However, the saturation of F intensity with the further increase of C_4F_8 appears to be related

[a)]Electronic mail: gyyeom@skku.edu

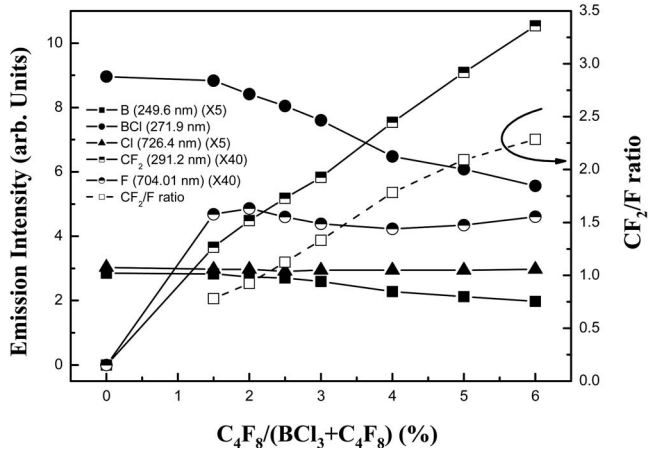

FIG. 1. OES intensities of B (249.6 nm), BCl (271.9 nm), Cl (724.6 nm), CF_2 (291.2 nm), F (704.01 nm), and CF_2/F ratio as a function of BCl_3/C_4F_8 gas mixtures. All the OES intensities were divided by the optical emission intensity of Ar (750.4 nm) [process conditions: Inductive power (700 W), dc bias voltage (−70 V), and operating pressure (12 mTorr)].

to the increased recombination with other radicals, such as CF, B, BCl, etc. Due to the saturation of F with increasing C_4F_8 percentage, the ratio of CF_2/F increased almost linearly with increasing C_4F_8 percentage.

Figure 2 shows the etch rate of ZrO_x, Si, PR, and their etch selectivities measured at the same process conditions in Fig. 1. The dc bias voltage to the substrate was maintained at −70 V. As shown in the figure, the etch rates of ZrO_x and Si with pure BCl_3 were 469 Å/min and 198 Å/min, respectively, therefore, the etch selectivity of ZrO_x/Si was 2.37. The small addition of C_4F_8 to BCl_3 upto 1.5% C_4F_8 increased the silicon etch rate to about 303 Å/min, however, the further addition of C_4F_8 to BCl_3 decreased the silicon etch rate monotonically and, when more than 3% C_4F_8 was added, deposition (shown as a negative etch rate) instead of etching occurred. In the case of ZrO_x, the small addition of C_4F_8 to 1.5% also increased the etch rate slightly and the further increase of C_4F_8 to 4% did not change the ZrO_x etch rate significantly. However, the addition of more than 4% C_4F_8 also decreased the etch rate and, by the addition of more than 6% C_4F_8, deposition instead of etching occurred. Therefore, by the addition of 3–4% C_4F_8, infinite etch selectivity could be obtained while maintaining a ZrO_x etch rate higher than 400 Å/min. In the case of the etch selectivity of ZrO_x to PR, as shown in the figure, the PR etch rate also decreased almost linearly and, by the addition of C_4F_8 more than 3%, a deposition on the PR layer instead of etching occurred, which was similar to the silicon surface. Therefore, infinite ZrO_x etch selectivity to PR could also be obtained using 3–4% C_4F_8.

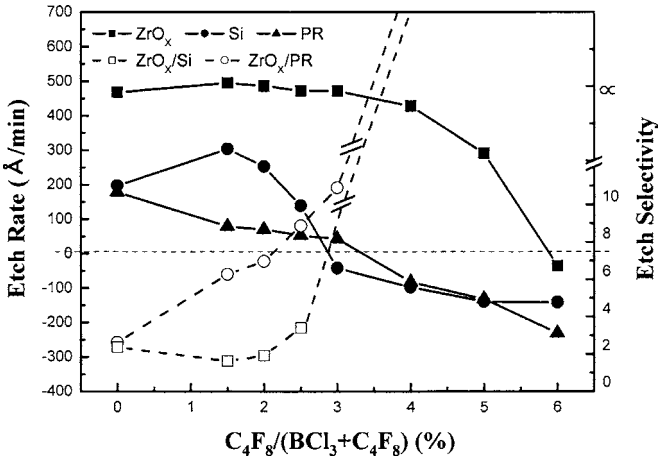

FIG. 2. Etch rates of ZrO_x, Si, and PR and etch selectivities of ZrO_x to Si and PR as a function of BCl_3/C_4F_8 gas mixtures [process conditions: inductive power (700 W), dc bias voltage (−70 V), and operating pressure (12 mTorr)].

The initial increase of the silicon etch rate observed with the addition of C_4F_8 upto 1.5% and the decrease of the silicon etch rate with a further increase of C_4F_8 in Fig. 2 appear to be related to the change of F and the ratio of CF_x/F in the plasma as shown in Fig. 1(b). The initial increase of F with addition of 1.5% C_4F_8 increased the silicon etch rate by forming volatile SiF_x, however, with further addition of C_4F_8 to BCl_3/C_4F_8, due to the increase of CF_2 and the ratio of CF_2/F, a thicker C–F polymer which acts as a protecting layer for chemical and physical etching[6–10] is formed on the silicon surface, therefore, the silicon etch rate is decreased and, finally, deposition instead of etching occurred when more than 3% of C_4F_8 is added. However, in the case of ZrO_x, in addition to the removal of oxygen in ZrO_x by the formation of volatile BCl_xO_y with BCl_x from BCl_3, the oxygen in ZrO_x is removed by forming volatile CO and CO_2 with carbon in C_4F_8. The ZrO_x surface is a Zr-rich surface forming volatile etch products such as ZrB_xCl_y and $ZrCl_x$ more easily. Therefore, the etch rate of ZrO_x did not change significantly until 4% C_4F_8 is added to the gas mixture because the decrease of ZrO_x etch rate by the decrease of BCl_3 percentage in the BCl_3/C_4F_8 gas mixture is compensated by the increase of ZrO_x etch rate through the removal of oxygen in ZrO_x by carbon in C_4F_8 and by preventing the formation of a thick C–F polymer on the ZrO_x surface.

Figure 3(a) shows the XPS data of oxygen on the ZrO_x surface before and after etching using BCl_3 and BCl_3/C_4F_8 (4%) and Fig. 3(b) shows the XPS data of carbon on the surfaces of ZrO_x and Si after etching using BCl_3/C_4F_8 (4%). The other process conditions were the same as those in Fig. 2. As shown in Fig. 3(a), the O 1*s* peak is divided into two peaks and the one at 530.27 eV is related to the Zr–O bonding, however, the other peak at 532.2 eV, whose intensity is similar before and after etching, appears to be related to the O–O bonding or oxygen bonding with contaminants formed during the air exposure before the XPS analysis. The oxygen atomic percentage related to the Zr–O bonding on the ZrO_x surface was 64% for as-deposited ZrO_x, however, after the etching of ZrO_x by pure BCl_3 and BCl_3/C_4F_8 (4%) plasmas, the percentage was decreased to 41% and 34%, respectively. The decrease of oxygen percentage on the ZrO_x surface during the etching by BCl_3 plasma is from the removal of oxygen in the ZrO_x by forming BCl_xO_y as mentioned earlier and the further decrease of oxygen during the etching by BCl_3/C_4F_8 plasma is from the further removal of oxygen in the ZrO_x by carbon in the C_4F_8. As shown in Fig. 3(b), the C 1*s* peak observed on the surfaces of ZrO_x by BCl_3/C_4F_8 (4%) plasma also showed two peaks related to C–C bond (284.5 eV) and C–Cl bond (286 eV) and, in the case of the etched silicon surface, in addition to the above peaks, a peak at 288.3 eV from the C–F bond was observed. The C–F bonding peak was observed due to the C–F polymer layer formed on the silicon surface, however, in the case of ZrO_x, no such C–F polymer layer was formed due to the removal of carbon from the CF_x in the C_4F_8 plasma by oxygen in the

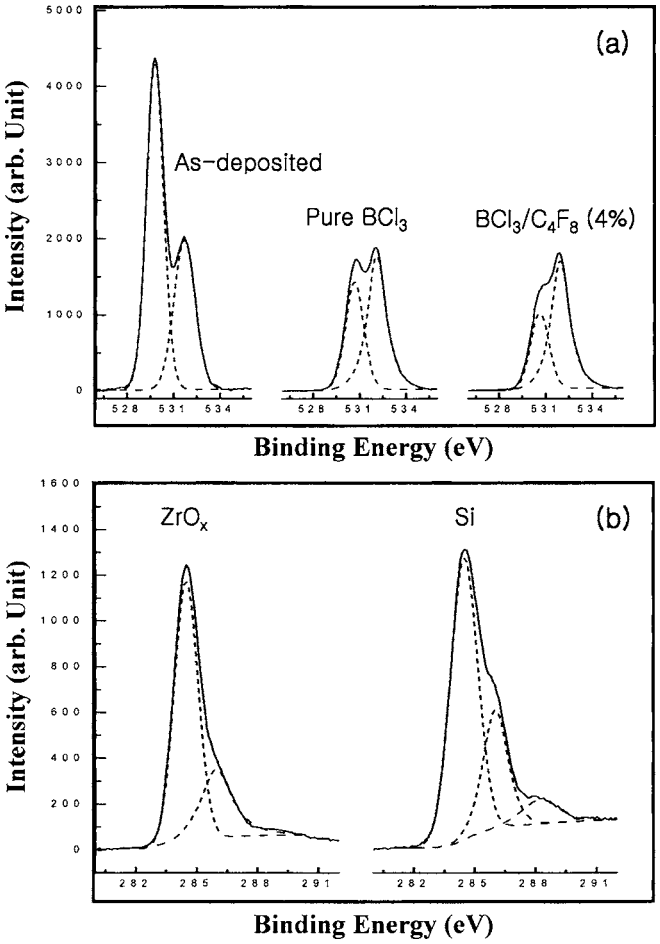

FIG. 3. XPS spectra of (a) O 1*s* narrow scan spectra of ZrO_x surface exposed to pure BCl_3, and BCl_3/C_4F_8 plasmas and (b) C 1*s* narrow scan spectra of ZrO_x and Si surface exposed to BCl_3/C_4F_8 plasma [process conditions: inductive power (700 W), dc bias voltage (−70 V), and operating pressure (12 mTorr)].

ZrO_x. However, as shown in Fig. 2, the increase of C_4F_8 in BCl_3/C_4F_8 higher than 4% will finally form a C–F polymer layer even on the ZrO_x surface. It is due to the fact that, with C_4F_8 higher than 4%, the flux of polymer forming CF_x arriving on the ZrO_x surface is higher than that can be removed by the oxygen in ZrO_x by forming CO_x, etc., and which results in the rapid decrease of ZrO_x etch rate with increasing C_4F_8 percentage as shown in Fig. 2.

Figure 4 shows SEM micrographs of ZrO_x observed after the etching followed by the PR removal. The process condition was 12 mTorr of BCl_3/C_4F_8 (4%), 700 W of inductive power, and −70 V of dc bias voltage. The etch time was 10 min corresponding to 20% of overetching time. As shown in the figure, only the ZrO_x layer was etched and no overetching into silicon was observed, therefore, a complete etch stop could be obtained.

In this study, using BCl_3/C_4F_8 plasmas, the etching characteristics of ZrO_x were investigated in addition to the

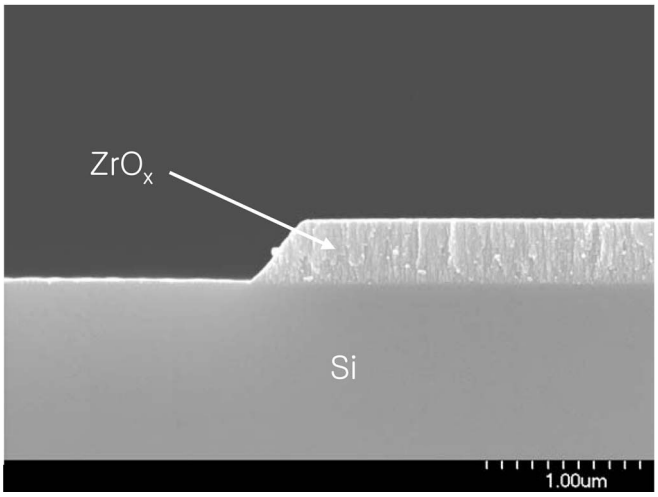

FIG. 4. Cross-sectional SEM micrographs of ZrO_x layer after the etching by BCl_3/C_4F_8 plasma [process conditions: Inductive power (700 W), dc bias voltage (−70 V), and operating pressure (12 mTorr)].

etch seletivities to Si. Also, using OES data and XPS data, the etching mechanism of ZrO_x by BCl_3/C_4F_8 was investigated. The increasing C_4F_8 in BCl_3/C_4F_8 mixture increased the etch selectivity of ZrO_x/Si without significantly changing the ZrO_x etch rate. The increased etch selectivity without changing the ZrO_x etch rate was obtained due to the formation of a C–F polymer on the silicon surface due to the increased CF_x flux to the substrate with increasing C_4F_8 percentage while no such C–F polymer was formed on the ZrO_x surface due to the removal of carbon from CF_x by the oxygen in ZrO_x. The infinite etch selectivities of ZrO_x to silicon and photoresit could be obtained by using BCl_3/C_4F_8 (3–4%) while maintaining ZrO_x etch rate above 400 Å/min.

This work supported by the National Program for 0.1 Terabit NVM Device and the National Research Laboratory Program (NRL) by the Korea Ministry of Science and Technology.

[1] A. I. Kingon, J. P. Maria, and S. K. Streiffer, Nature (London) **406**, 1032 (2000).
[2] B. O. Cho, J. Wang, L. Sha, and J. P. Chang, Appl. Phys. Lett. **80**, 1052 (2002).
[3] L. Sha and J. P. Chang, J. Vac. Sci. Technol. A **21**, 1915 (2003).
[4] L. Sha and J. P. Chang, J. Vac. Sci. Technol. A **22**, 88 (2004).
[5] D. W. Kim, C. H. Jeong, K. N. Kim, H. Y. Lee, H. S. Kim, Y. J. Sung, and G. Y. Yeom, Thin Solid Films **435**, 242 (2003).
[6] D. Zhang and M. J. Kushner, J. Vac. Sci. Technol. A **19**, 524 (2000).
[7] C. J. Mogab, A. C. Adams, and D. L. Flamm, J. Appl. Phys. **49**, 3796 (1983).
[8] K. Takahashi, M. Hori, S. Kishimoto, and T. Goto, Jpn. J. Appl. Phys., Part 1 **33**, 4181 (1994).
[9] F. H. Bell, O. Joubert, G. S. Oehlein, Y. Zhang, and D. Vender, J. Vac. Sci. Technol. A **12**, 3095 (1994).
[10] L. Rolland, M. C. Peignon, Ch. Cardinaud, G. Turban, Microelectron. Eng. **53**, 375 (2000).